Final Draft
of the original manuscript:

Wang, F.F.; Li, W.Y.; Shen, J.; Wen, Q.; dos Santos, J.F.:
Improving weld formability by a novel dual-rotation bobbin tool friction stir welding
In: Journal of Materials Science and Technology (2017) Elsevier

DOI: 10.1016/j.jmst.2017.11.001

Improving weld formability by a novel dual-rotation bobbin tool friction stir welding

F.F. Wang [1, 2, 3], W.Y. Li [1,**], J. Shen [2,*], Q. Wen [1], J.F. dos Santos [2]

[1] *State Key Laboratory of Solidification Processing, Shaanxi Key Laboratory of Friction Welding Technologies, Northwestern Polytechnical University, Xi'an 710072, Shaanxi, PR China*

[2] *Helmholtz-Zentrum Geesthacht, Institute of Materials Research, Materials Mechanics, Geesthacht 21502, Germany*

[3] *China Academy of Launch Vehicle Technology, Beijing Institute of Astronautical Systems Engineering, Beijing 100076, PR China*

[Received 5 March 2017; Received in revised form 10 April 2017]

Corresponding authors:

** W.Y. Li, Tel.: ++86-29-88495226, Fax: ++86-29-88491426,

Email address: liwy@nwpu.edu.cn (W.Y. Li)

* J. Shen, Tel.:++49-0415287-2074, Fax: ++49-0415287-2050,

Email address: junjun.shen@hzg.de (J. Shen)

A novel dual-rotation bobbin tool friction stir welding (DBT-FSW) was developed, in which the upper shoulder (US) and lower shoulder (LS) have different rotational speeds. This process was tried to weld 3.2 mm thick aluminum-lithium alloy sheets. The metallographic analysis and torque measurement were carried out to characterize the weld formability. Experimental results show that compared to conventional bobbin tool friction stir welding, the DBT-FSW has an excellent process stability, and can produce the defect-free joints in a wider range of welding parameters. These can be attributed to the significant improvement of material flow caused by the formation of a staggered layer structure and the unbalanced force between the US and LS during the DBT-FSW process.

Keywords: Bobbin tool friction stir welding; Dual rotation; Material flow; Microstructure; Microhardness

1. Introduction

As has been well described in numerous publications, friction stir welding (FSW) can produce welds that are free of defects associated with local melting and solidifcation, which are characteristics of the traditional fusion welding processes [1-3]. Since FSW is a solid state process, weldability can be significantly improved in certain materials, such as high strength aluminum alloys, steels and metal matrix composites [4-6]. However, owing to the typically high down forces needed in the process, FSW is usually practiced as a fully mechanized process, and a rigid anvil support from the bottom surface of the workpiece is generally inevitable, which reduces the application of FSW in complex structures [7,8].

Bobbin tool friction stir welding (BT-FSW) is an enhancement and another good variant of FSW, using a welding tool with a upper shoulder (US) and lower shoulder (LS) connected by a probe [9,10]. It has been declared that BT-FSW has high potential in welding of closed profiles [11]. However, there are many scientific questions for this young technology [12]. Among them the most common problem reported is the void and tunnel defects [12,13]. Although defect-free joints can be obtained by the well-designed probe feature and optimized welding parameters [12], some investigations proved that unexpected void and tunnel defects do present in a regular welding parameter [14,15]. These defects are often considered as a consequence of inappropriate material flow and insufficient mixing during welding [16,17].

An effective methodology for enhancing the material flow in BT-FSW is therefore in ever demand. It has been proved that the dual-rotation setup can effectively improve the material flow on FSW [3,18,19]. Inspired by that finding, therefore, a novel dual-rotation BT-FSW (DBT-FSW) was developed, in which the US and LS have different rotational speeds, to obtain Al-Li alloy AA2198-T851 sheets. Preliminary experiments show that the DBT-FSW process greatly improves material flow and effectively avoids the void defect. Therefore, the present work is to reveal the essential reason for the improved weld formability during DBT-FSW.

2. Experimental procedure

Aluminum-lithium alloy (AA2198-T851) sheets with dimensions of 250×100×3.2 mm were butt-welded by both BT-FSW and DBT-FSW along the rolling direction at a welding speed (v) of 42 mm/min and the rotational speeds (ω) from 400 to 1200 rpm. The welding tool was characterized by a cylinder featureless probe (Ø4 mm) and a concave shoulder (Ø11 mm) as shown in Fig. 1a. The LS was attached to the probe and driven by a motor shaft, while the US was rotated by another independent motor, therefore making the US and LS can have the same (i.e., BT-FSW) and different (i.e., DBT-FSW) rotational speeds. The welding system can adjust both the gap and gap force F_{gap} (i.e. distance and force between the US and LS) induced on the workpiece. Also, the reacting torque/force was measured by an embedded torque/force measuring system in the custom designed FSW (Flexi Stir) machine. At the beginning of the welding process, the plunge depth was set as 0.1mm for both US and LS. After the controlling model shifted to force control model, the plunge depth various with the gap force, and all joints showed good surface appearance for both BT-FSW and DBT-FSW.

Samples for microstructure analysis were cut perpendicular to the welding direction, mechanically ground and polished, etched using the Keller's Reagent (2 ml HF, 3 ml HCl, 5 ml HNO_3, and 190 ml H_2O), and examined by optical microscopy (OM). A suitable surface finish for electron backscatter diffraction (EBSD) was achieved by applying mechanical polishing in a similar fashion followed by vibration polishing. The hardness maps of the cross sections were obtained using an UTS100 hardness tester with a load of 0.2 kg for 10 s. The 2D hardness map was consisting of 11 lines on the cross sections with point space of 0.25mm and line space of 0.25mm.

3. Results and discussion

3.1 Formation mechanism

Figs. 2a and 2b show the transverse cross-section of the BT-FSW joint produced at rotational speed of 600rpm, and the DBT-FSW joint produced at the US rotational speed of 400rpm and LS rotational speed of 600rpm, respectively. Both of them have an hourglass shaped stirred zone (SZ), composing of the US dominated zone (USDZ) and LS dominated zone (LSDZ) [10]. The distinct microstructures lead to an obvious triple junction of thermo-mechanically affected zone (TMAZ), USDZ and LSDZ on the advancing side (AS) of the joint [20]. Moreover, compared to BT-FSW, DBT-FSW has a much wider TMAZ with waved structure as shown in Figs. 2d and 2e. However,

similar to other reports [14,15], the unexpected void defect sometimes happens even using the same welding parameters in BT-FSW at the triple junction as shown in Fig. 2c. A series of welding experiments are repeated with increasing rotational speeds from 400 to 1200 rpm. Unfortunately, the void defect is found at all rotational speeds and is very difficult to be eliminated as shown in Fig. 3a, indicating a poor stability of BT-FSW. By contrast, no void defect is found in the DBT-FSW joint at rotational speeds from 400 to1200 rpm as shown in Fig. 3b. These facts reveal a good weld formability and stability of DBT-FSW. This improvement of the weld quality by DBT-FSW should be attributed to the following reasons.

On one hand, DBT-FSW generates an asymmetrical material flow with staggered layer structure in the weld, which makes the voids can be easily filled during welding. As can be observed from the material flow pattern at the run-out of DBT-FSW, two parts of periodical layer structures emerge on the cross section in the USDZ and LSDZ, respectively, as shown in Fig. 4a. The layer structure comes from a cyclic material deposition in the wake of the weld, causing by a dynamic contact condition between the tool and the matrix [21,22]. The periodic distance (λ) between each layer corresponds with the ratio of v/ω [23,24]. In BT-FSW, the layer structures of the USDZ and LSDZ have the same λ value and their crests and troughs collide synchronous at the triple junction region (see Fig. 4c). Apparently, some big voids are left between the troughs of the USDZ and LSDZ and are difficult to be filled during welding, probably resulting in the void defect. However, in DBT-FSW, the λ value is different between the USDZ and LSDZ (see Fig. 4d). The LSDZ has a smaller λ than that of the USDZ due to the higher rotational speed [23,24]. This means that the crests and troughs are staggered between the USDZ and LSDZ, which significantly decreases the cavity size compared to that of the BT-FSW. Thus the void defect can be more easily avoided in DBT-FSW.

On the other hand, DBT-FSW generates an unbalanced force between the US and LS, making more sufficient material flow in the thickness direction of the joint. This unbalanced force can be shown by the measured torque in the US (M_{us}) and LS (M_{ls}) (see Fig. 4b) and the deformed microstructure in the joint (see Figs. 4c and 4d). In BT-FSW, the M_{us} are almost the same as M_{ls}, indicating a balanced force between the US and LS [10,11,20]. This leads to a weak and symmetric material flow in the joint's thickness direction, and the resultant narrow TMAZ and void defect. Moreover, it is very difficult to improve the material flow in this direction by increasing the heat input [14,15,20]. By contrast, in DBT-FSW, significantly different M_{us} and M_{ls}, and a wide waved

structure in TMAZ are observed in Figs. 2d and 4d. Those facts reveal an intense material flow in thickness direction of the joint under the unbalanced force. Apparently, DBT-FSW effectively avoids the void defect at the triple junction of TMAZ, USDZ and LSDZ, due to the improved material flow.

All results suggest that DBT-FSW leads to more sufficient material flow and mixing than BT-FSW. Therefore, the defect-free joint can be more easily obtained by DBT-FSW than by BT-FSW in a wider range of welding parameters. It is believed that the DBT-FSW could have a better industrial adaptability in the future.

3.2 Typical microstructure of DBT-FSW joint

In order to further describe the characteristics of the asymmetric weld formation, the typical microstructure of the DBT-FSW joint was well investigated on the joint produced at different rotational speeds of US and LS. Fig. 5 shows the microstructures in the SZ along the weld center line of the joint (from the top to the bottom surfaces), where the rotational speeds of US and LS are 400 rpm and 100rpm and the welding speed is 42mm/min. In the previous work by Shen et al. [10] and Wang et al. [20], a thorough investigation on BT-FSW of 3.2mm thick 2198-T8 alloy has been done. The macrostructure along the joint cross section are quite similar between BT-FSW and DBT-FSW (see Fig. 2). Hereby, Fig. 5 only shows the grain size and high-angle grain boundaries (HAGB) in the stirred zone (SZ) of the joint. It can be clearly seem from Fig. 5d that there is the difference between the USDZ and LSDZ.

3.3 Microhardness of DBT-FSW joint

Fig. 6 shows the 2D hardness map and the mid-thickness hardness profile of the weld. It is clear that a roughly symmetrical hardness distribution is obtained in the thickness direction. The lowest hardness zone is clearly shown at the edge regions of the shoulder. A typical W-shaped hardness profile is observed along the cross section. Apparently, the hardness drops significantly in the DBT-FSWed AA2198-T851 alloy. The highest hardness exhibits in the BM, and the hardness rises above 104 Hv within the SZ after reaching a minimum 100 Hv at the HAZ, which indicates the W-shaped hardness profile. Same as the reports in BT-FSW of Al-Li alloy, this hardness softening throughout weld zone is principally related to the coarsening and dissolution of

precipitates in Al-Li alloys during welding caused by the thermal cycle and plastic deformation [25,26]. The sharp hardness drop in the BT-FSWed AA2198-T851 is caused by the coarsening and dissolution of the precipitates from the HAZ to the SZ. On the other hand, the hardness is almost symmetrical in the thickness direction, which could be the result of the balanced heat generation and the thin BM. At last, the softest region (minimum hardness) always locates in the TMAZ or in the HAZ in BT-FSWed and FSWed high-strength aluminum alloys [25,26], which is always related to the fracture location and morphology of the joint under loading.

4. Conclusions

Compared to BTFSW, the newly developed DBT-FSW has high process stability and can produce the defect-free joints in a wider range of welding parameters. DBT-FSW creates a staggered layer structure and unbalanced force between the US and LS, making more sufficient material flow in the joint's thickness direction. The improved material flow effectively avoids the formation of void defect at the triple junction of TMAZ, USDZ and LSDZ. The asymmetric grain size and the fraction of high-angle grain boundaries in the thickness direction are significantly introduced by DBT-FSW while a very slight change is found in the thin plate joints. Further work is still necessary to facilitate its industrial applications.

Acknowledgements

Feifan Wang would like to acknowledge the China Scholarship Council (No. 201306290117) for the financial support. This work has been carried out under the auspices of the Cooperation Agreement between the School of Material Sciences and Engineering of the Northwestern Polytechnical University and the Helmholtz-Zentrum Geesthacht (HZG 161/2014 and 111 Project/B08040).

References

[1] X.X. Zhang, D.R. Ni, B.L. Xiao, H. Andrä, W.M. Gan, M. Hofmannd, Z.Y. Ma, Acta Mater. 87 (2015) 161-173.

[2] R.Z. Xu, D.R. Ni, Q. Yang, C.Z. Liu, Z.Y. Ma, J. Mater. Sci. Technol. 32 (2016) 76-88.

[3] J.Q. Li, H.J. Liu, J. Mater. Sci. Technol. 31 (2015) 375-383.

[4] L.Wan, Y.X. Huang, W.Q. Guo, S.X. Lv, J.C. Feng, J. Mater. Sci. Technol. 30 (2014) 1243-1250.

[5] G.M. Xie, H.B. Cui, Z.A. Luo, W. Yu, J. Ma, G.D. Wang, J. Mater. Sci. Technol. 32 (2016) 326-333.

[6] H.J. Liu, Y.Y. Hu, Y.Q. Zhao, Mater. Lett. 158 (2015) 136-139.

[7] D.R. Ni, J.J. Wang, Z.Y. Ma, J. Mater. Sci. Technol. 32 (2016) 162-166.

[8] Y.M. Yue, Z.W. Li, S.D. Ji, Y.X. Huang, Z.L. Zhou, J. Mater. Sci. Technol. 32 (2016) 671-675.

[9] W.M. Thomas, C.S. Wiesner, D.J. Marks, D.G. Staines, Sci. Technol. Weld. Join. 14 (2009) 247-253.

[10] J. Shen, F. Wang, U.F.H. Suhuddin, S. Hu, W. Li, J.F. dos Santos, Metall. Mater. Trans. A 46 (2015) 2809-2813.

[11] P.L. Threadgill, M.M.Z. Ahmed, J.P. Martin, J.G. Perrett, B.P. Wynne, Mater. Sci. Forum 638-642 (2010) 1179-1184.

[12] M.K. Sued, D. Pons, J. Lavroff, E.H. Wong, Mater. Des. 54 (2014) 632-643.

[13] H.J. Liu, J.C. Hou, H. Guo, Mater. Des. 50 (2013) 872-878.

[14] L. Wan, Y. Huang, Y. Wang, S. Lv, J. Feng, Mater. Sci. Technol. 31 (2015) 1433-1442.

[15] W.Y. Li, T. Fu, L. Hütsch, J. Hilgert, F.F. Wang, J.F. dos Santos, N. Huber, Mater. Des. 64 (2014) 714-720.

[16] R. Nandan, T. Debroy, H. Bhadeshia, Prog. Mater. Sci. 53 (2008) 980-1023.

[17] A.P. Reynolds, Scr. Mater. 58 (2008) 338-342.

[18] W.M. Thomas, I.M. Norris, D.G. Staines, P.J. Clarke, N.L. Horrex, The 1st International Conference 'Joining of aluminium structures', Moscow, Russian, December 3-5, 2007.

[19] J.Q. Li, H.J. Liu, Mater. Des. 45 (2013) 148-154.

[20] F.F. Wang, W.Y. Li, J. Shen, S.Y. Hu, J.F. dos Santos, Mater. Des. 86 (2015) 933-940.

[21] H.N.B. Schmidt, T.L. Dickerson, J.H. Hattel, Acta Mater. 54 (2006) 1199-1209.

[22] G.R. Cui, Z.Y. Ma, S.X. Li, Acta Mater. 57 (2009) 5718-5729.

[23] Z.W. Chen, T. Pasang, Y. Qi, Mater. Sci. Eng. A 474 (2008) 312-316.

[24] J.W. Qian, J.L. Li, J.T. Xiong, F.S. Zhang, W.Y. Li, X. Lin, Sci. Technol. Weld. Join. 17 (2012) 338-341.

[25] T.L. Jolu, T.F. Morgeneyer, A.F. Gourgues-Lorenzon, Sci. Technol. Weld. Join. 15 (2010)

694-698.

[26] F.F. Wang, W. Y. Li, J. Shen, Z.H. Zhang, J.L. Li, J. F. J. dos Santos, Sci. Technol. Weld. Join. 21 (2016) 479-483.

Figure captions

Fig. 1. (a) Details of the welding tool and (b) schematic of DBT-FSW.

Fig. 2. OM images of: (a) BT-FSW joint; (b) DBT-FSW joint; (c) typical void defect exhibited in BT-FSW; and typical microstructure on the AS of (d) DBT-FSW and (e) BT-FSW.

Fig. 3. Welding parameter windows of (a) BT-FSW and (b) DBT-FSW.

Fig. 4. (a) Layer structure at the run-out of the DBT-FSW joint; (b) measured torque of the welding tool; and illustration for material flow in (c) BT-FSW and (d) DBT-FSW.

Fig. 5. Microstructures in the SZ along the weld center line of DBT-FSW joint: (a) 0.2mm; (b) 1.35mm; (c) 1.81mm; (d) grain size and fraction of HAGB.

Fig. 6. Microhardness distribution on the cross-section of typical DBT-FSW joint.

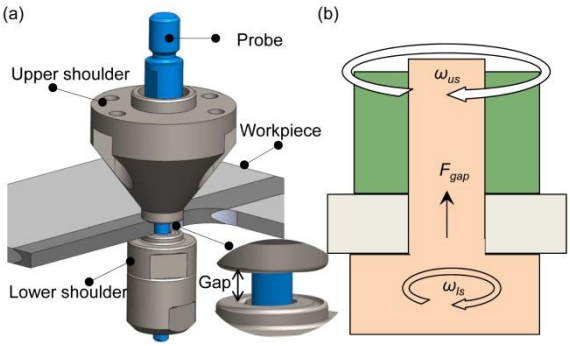

Fig. 1. (a) Details of the welding tool and (b) schematic of DBT-FSW.

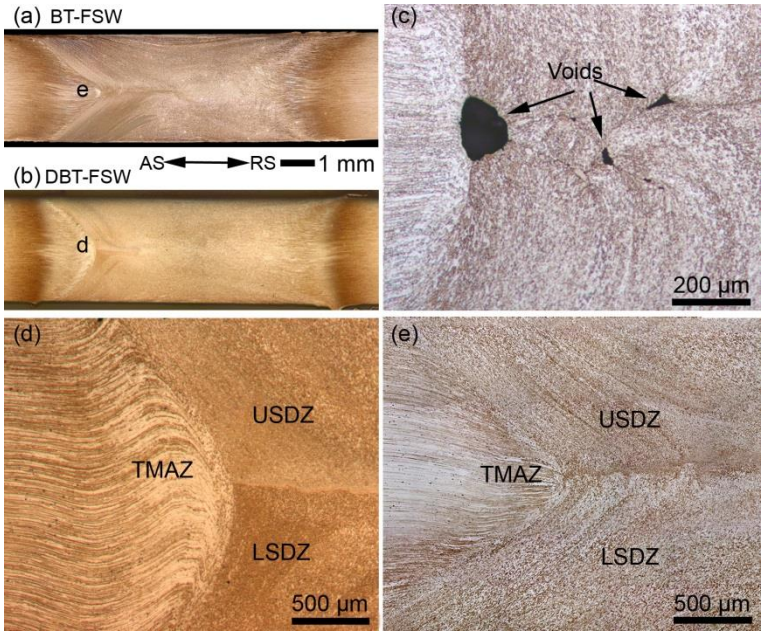

Fig. 2. OM images of: (a) BT-FSW joint; (b) DBT-FSW joint; (c) typical void defect exhibited in BT-FSW; and typical microstructure on the AS of (d) DBT-FSW and (e) BT-FSW.

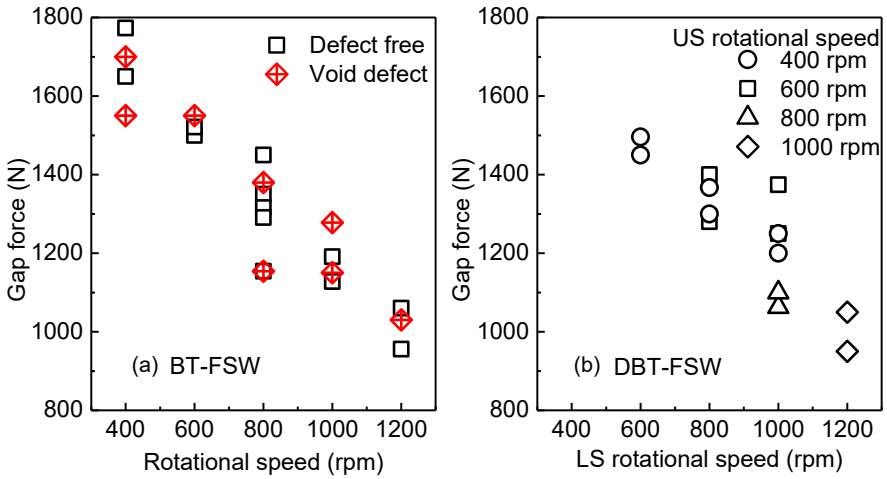

Fig. 3. Welding parameters windows of (a) BT-FSW and (b) DBT-FSW.

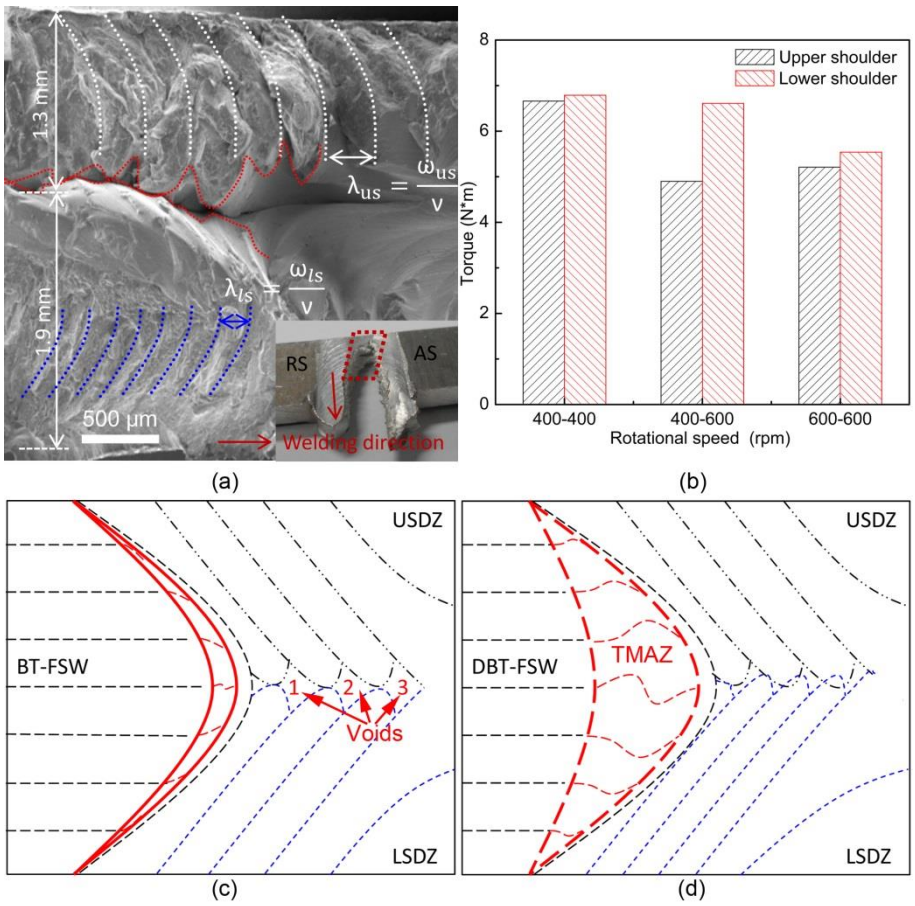

Fig. 4. (a) Layer structure at the run-out of the DBT-FSW joint; (b) measured torque of the welding tool; and illustration for material flow in (c) BT-FSW and (d) DBT-FSW.

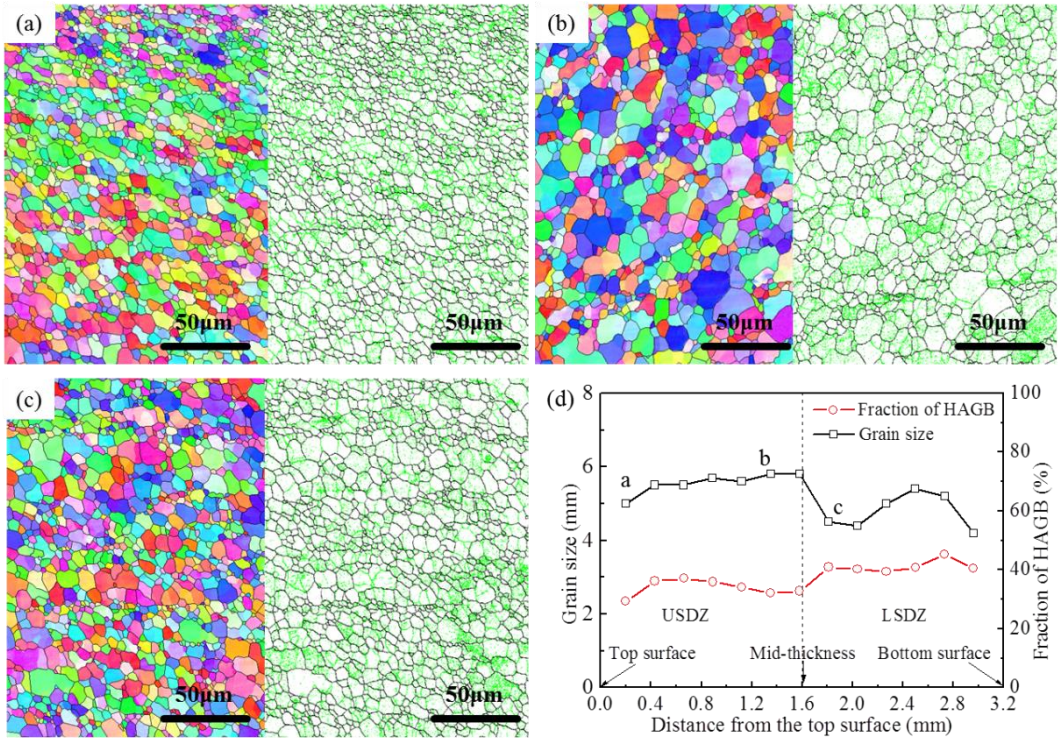

Fig. 5. Microstructures in the SZ along the weld center line of DBT-FSW joint: (a) 0.2mm; (b) 1.35mm; (c)

1.81mm; (d) grain size and fraction of HAGB.

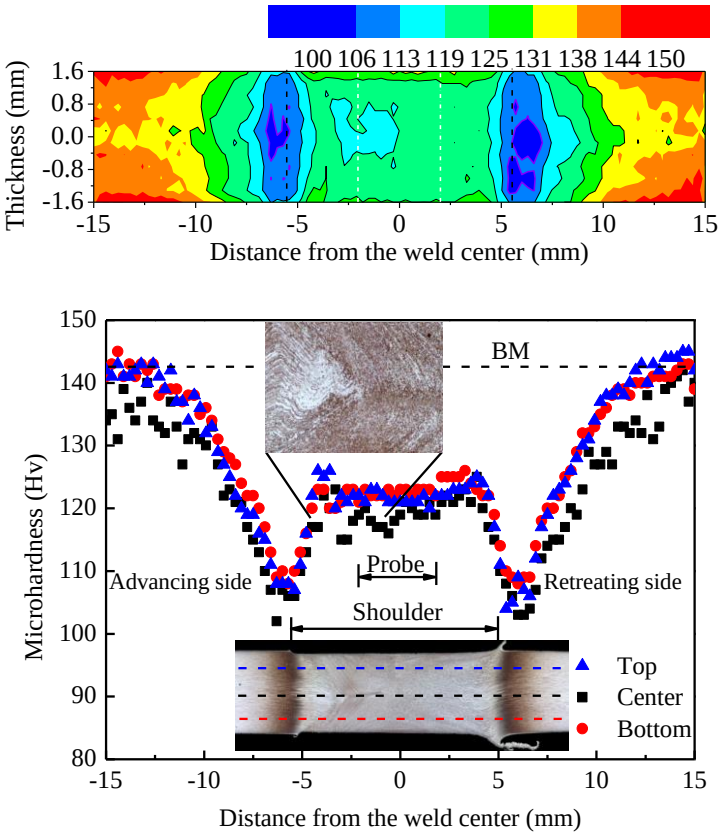

Fig. 6. Microhardness distribution on the cross-section of typical DBT-FSW joint.